Electronic Supplementary Information for

A One-step, Cost-effective Green Method to *in situ* Fabricate $Ni(OH)_2$ Hexagonal Platelets on Ni Foam as Binder-Free Supercapacitor Electrode Materials

Lingjie Li,‡[a,b] Jing Xu,‡[a] Jinglei Lei,*[a,b] Jie Zhang,[a] Frank McLarnon,[a] Zidong Wei,[a,b] Nianbing Li,[c] Fusheng Pan[d]

[a] *School of Chemistry and Chemical Engineering, Chongqing University, Chongqing, 400044, PR China. E-mail: JLLei@cqu.edu.cn; Fax: +86 2365112328; Tel: +86 13983064116*
[b] *Chongqing Key Laboratory of Chemical Process for Clean Energy and Resource Utilization, Chongqing University, Chongqing, 400044, PR China*
[c] *School of Chemistry and Chemical Engineering, Southwest University, Chongqing, 400715, PR China*
[d] *School of Materials Science and Engineering, Chongqing University, Chongqing, 400044, PR China*

S1. Mass measurement and calculation

The weight of a sample was measured using a Mettler Toledo XS205DU microbalance (0.01 mg sensitivity). Before weighing, all samples were thoroughly dried in a vacuum oven until the mass displayed no variation. The loading mass of the $Ni(OH)_2$ active materials can be obtained by measuring the weight change of the samples before and after hydrothermal process and calculating according to the following equation:[1]

$$m = C * (m_2 - m_1)$$

where m is the loading mass of the $Ni(OH)_2$ active materials, m_1 is the mass of the Ni foam before hydrothermal process and m_2 is the mass of the sample after hydrothermal process, C is a constant which represents the molar mass ratio of $\frac{M_{Ni(OH)_2}}{M_{Ni(OH)_2} - M_{Ni}}$. The mass loading of the active material $Ni(OH)_2$ in the work is ~3.00 mg/cm^2.

S2. Electrochemical specific capacitance calculation

Calculation of specific capacitance (C_s, F g^{-1}) in this work is based upon subtraction of the capacitance which belongs to the Ni foam current collector from the total capacitance of the as-prepared HNF electrode according to following equations:

(1) based upon the CV curves:[2-6]

$$C_s = \frac{Q_{HNF} - Q_{\text{Ni foam}}}{\Delta V \times m_{Ni(OH)_2}} = \frac{1}{v \times m_{\text{Ni(OH)}_2} \times (V_c - V_a)} \left[\int_{V_a}^{V_c} i_{HNF}(V)dV - \int_{V_a}^{V_c} i_{\text{Ni foam}}(V)dV \right]$$

where $m_{\text{Ni(OH)}_2}$ is the mass of the $Ni(OH)_2$ electroactive material in the HNF electrode (g), v is the potential scan rate (V s^{-1}), V_a is the anodic potential (V), V_c is the cathodic potential (V), $i(V)$ is the response current density (A) and V is the potential (V).

(2) based upon the galvanostatic charge-discharge curves:[2,4-8]

$$C_s = \frac{I \times \Delta t_{HNF} - I \times \Delta t_{\text{Ni foam}}}{m_{Ni(OH)_2} \times \Delta V}$$

where I is the discharge current (A), Δt is the discharge time (s), $m_{\text{Ni(OH)}_2}$ is the mass of the $Ni(OH)_2$ electroactive material in the HNF electrode (g) and ΔV is the potential change during discharge (V).

(3) based upon the EIS analysis:[9-12]

$$C_s = \frac{1}{2\pi f Z''}$$

where f is the frequency (Hz), Z'' is the imaginary part of the complex impedance Z (Ω cm^2).

S3. Contribution of Ni foam collector to HNF electrode electrochemical performance

In order to evaluate the contribution of Ni foam collector in the electrochemical measurement, CV curves and galvanostatic charge-discharge curves of a blank Ni foam collector with the same working area were measured under identical conditions, and the results are presented in Fig. S1 and Fig. S2. Comparisons with those of the as-prepared HNF electrode are presented in Fig. S3 and Fig.

S4. Obviously, the contribution of the blank Ni foam collector in the electrochemical measurement is very small (~4.0% in CV measurements and ~1.3% in galvanostatic charge-discharge tests).

Supplementary Figures and Table

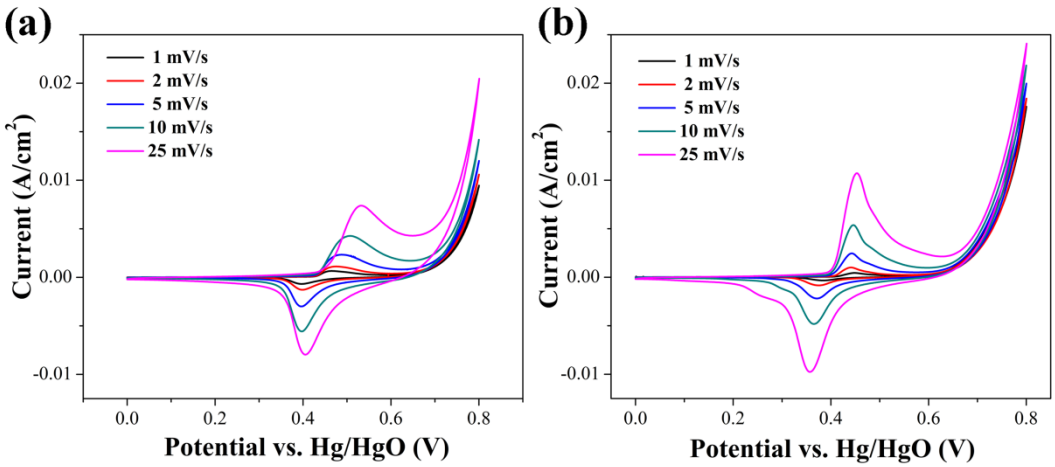

Fig. S1 CV curves of the blank Ni foam collector at various scan rates in (a) 1.0 M KOH and (b) 2.0 M KOH aqueous solution.

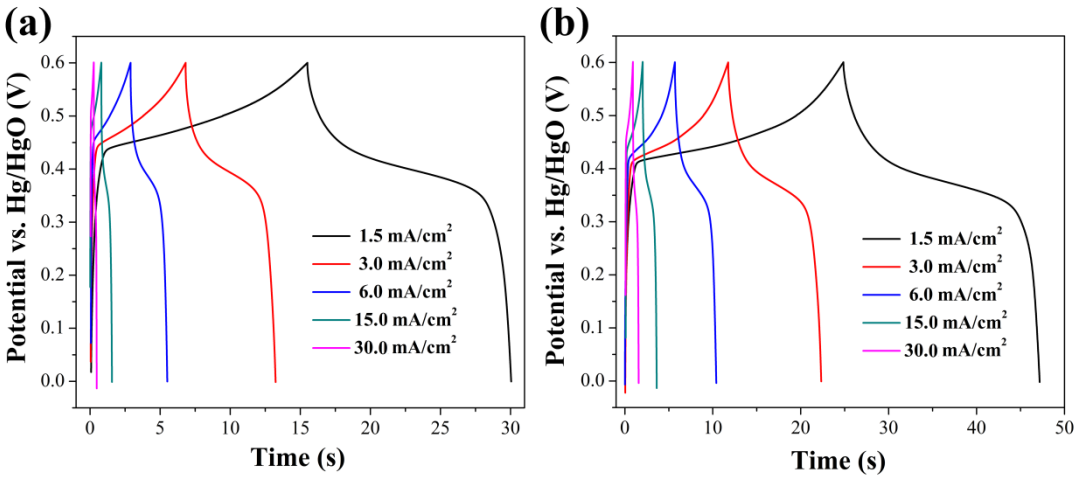

Fig. S2 Galvanostatic charge-discharge curves of the blank Ni foam collector at various current densities in (a) 1.0 M KOH and (b) 2.0 M KOH aqueous solution.

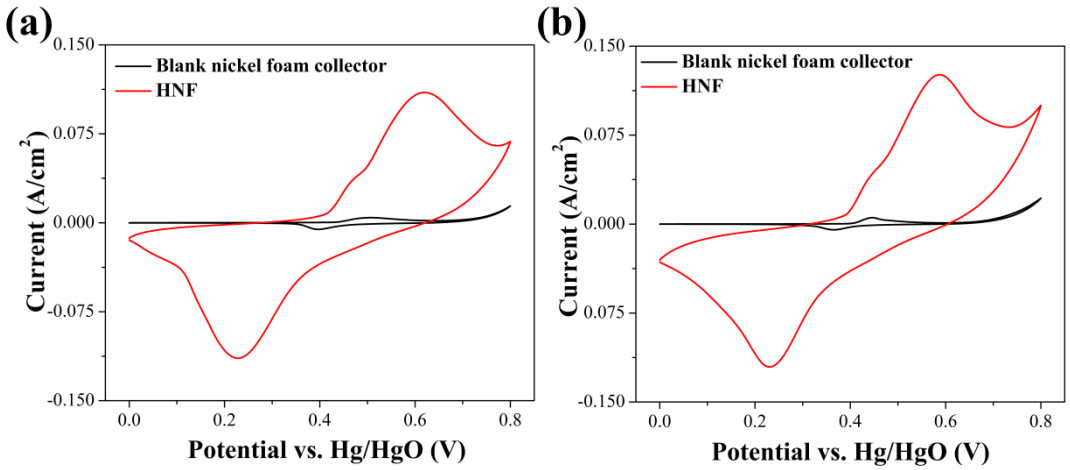

Fig. S3 Comparison of CV curves of the blank Ni foam collector and the as-prepared HNF electrode at a scan rate of 10 mV s^{-1} in (a) 1.0 M KOH and (b) 2.0 M KOH aqueous solution.

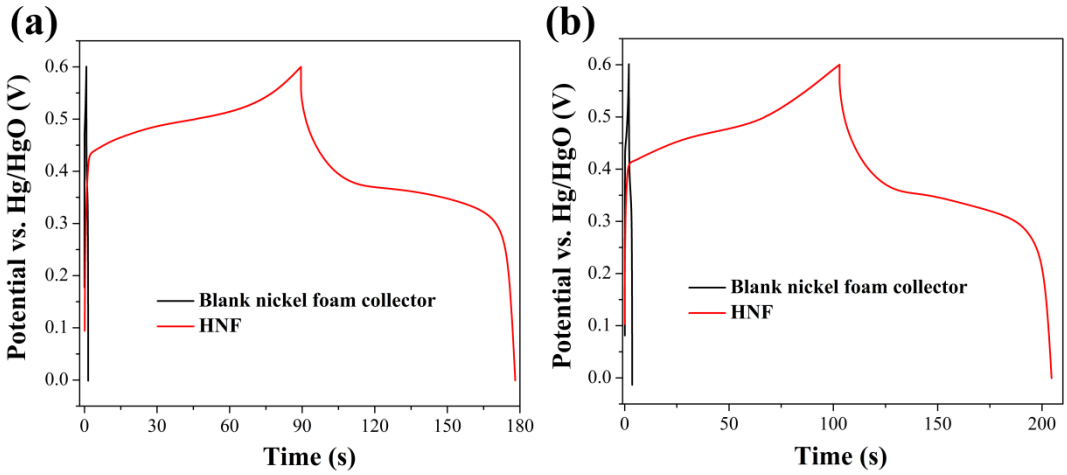

Fig. S4 Comparison of galvanostatic charge-discharge curves of the blank Ni foam collector and the as-prepared HNF electrode at current density of 5 A g^{-1} in (a) 1.0 M KOH and (b) 2.0 M KOH aqueous solution.

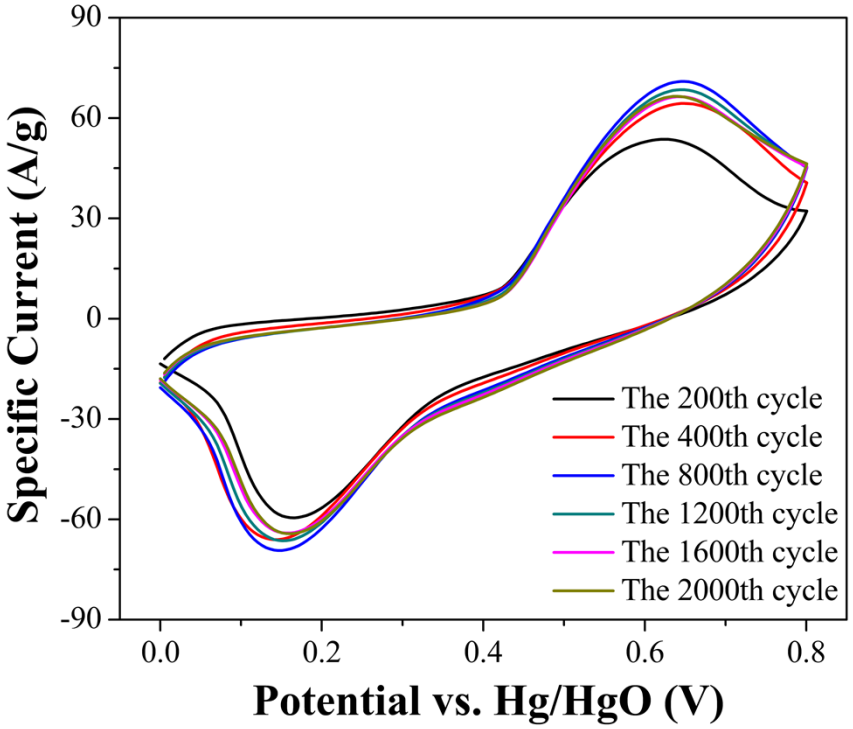

Fig. S5 CV curves of some cycles during the cyclic performance test (scan rate: 50 mV s^{-1}).

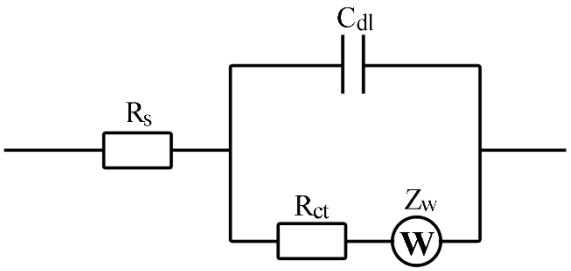

Fig. S6 Equivalent electrical circuit used for fitting the EIS result shown in Fig. 7. R_s is the equivalent series resistance, C_{dl} is the double-layer capacitance, R_{ct} is the charge transfer resistance, and Z_W is the Warburg impedance.

Table S1. Comparison of the fabrication process and electrochemical performance of the as-prepared $Ni(OH)_2$ material in this work with those reported in previous literatures.

Ref.	Active material	Nickel element source	Fabrication technique	Specific capacitance	Capacitance stability after cycling
This work	$Ni(OH)_2$ platelets	Nickel foam	Hydrothermal	2534 F g^{-1} at 1 mV s^{-1}	97% at 50 mV s^{-1} after 2000 cycles
13	$Ni(OH)_2$ thin film	$Ni(NO_3)_2$	Hydrothermal	357 F g^{-1} at 5 mV s^{-1}	82% at 100 mV s^{-1} after 500 cycles
14	$Ni(OH)_2$ microspheres	$NiCl_2$	Hydrothermal	1028.5 F g^{-1} at 2.22A g^{-1}	100% at 3.7 A g^{-1}after 1000 cycles
15	$Ni(OH)_2$ thin film	$NiCl_2$	Chemical vapor deposition	166 F g^{-1} at 0.5 A/ g^{-1}	65% at 10 A g^{-1} after 1000 cycles
16	$Ni(OH)_2$ nanoflakes	$Ni(NO_3)_2$	Coprecipitation	1780 F g^{-1} at 1 A g^{-1}	88% at 5 A g^{-1} after 500 cycles
17	$Ni(OH)_2$ microspheres	$Ni(NO_3)_2$	Hydrothermal	1788.9 F g^{-1} at 0.5 A g^{-1}	85 % at 0.5 A g^{-1} after 500 cycles
18	$Ni(OH)_2$ nanobelts	$Ni(Ac)_2$	Hydrothermal	755 F g^{-1} at 1 A g^{-1}	93% at 10 A g^{-1} after 500 cycles
19	$Ni(OH)_2$ nanoplates	$Ni(NO_3)_2$	Hydrothermal	793 F g^{-1} at 1 A g^{-1}	
20	$Ni(OH)_2$ nanoparticles	$NiCl_2$	Cathodic electrodeposition	740 F g^{-1} at 10 mV s^{-1}	
21	$Ni(OH)_2$ nanowalls	$Ni(NO_3)_2$	Hydrothermal	2675 F g^{-1} at 5mA cm^{-2}	96% at 30 mA cm^{-2} after 500 cycles
22	$Ni(OH)_2$ thin film	$Ni(NO_3)_2$	Chemical bath deposition	398 F g^{-1} at 5 mV s^{-1}	
23	$Ni(OH)_2$ particles	$Ni(NO_3)_2$	Chemical precipitation	314.5 F g^{-1} at 2 mV s^{-1}	

References

1 C. Tang, X. Yin, H. Gong, ACS Appl. Mater. Interfaces, 2013, **5**, 10574.

2 H. B. Li, M. H. Yu, F. X. Wang, P. Liu, Y. Liang, J. Xiao, C. X. Wang, Y. X. Tong, G. W. Yang, Nature Commun., 2013, **4**, 1894.

3 J. Yan, Z. Fan, W. Sun, G. Ning, T. Wei, Q. Zhang, R. Zhang, L. Zhi, F. Wei, Adv. Funct. Mater., 2012, **22**, 2632.

4 S. W. Lee, J. Kim, S. Chen, P. T. Hammond, Y. Shao-Horn, ACS Nano, 2010, **4**, 3889.

5 S. Dong, X. Chen, L. Gu, X. Zhou, L. Li, Z. Liu, P. Han, H. Xu, J. Yao, H. Wang, X. Zhang, C. Shang, G. Cui, L. Chen, Energy Environ. Sci., 2011, **4**, 3502.

6 Z. Yu, J. Thomas, Adv. Mater., 2014, **26**, 4279.

7 B. Wang, J. S. Chen, Z. Wang, S. Madhavi, X. W. Lou, Adv. Energy Mater., 2012, **2**, 1188.

8 Q. Lu, M. W. Lattanzi, Y. Chen, X. Kou, W. Li, X. Fan, K. M. Unruh, J. G. Chen, J. Q. Xiao, Angew. Chem. Int. Ed., 2011, **50**, 6847.

9 S. Vijayakumar, S. Nagamuthu, G. Muralidharan, ACS Appl. Mater. Interfaces, 2013, 5, 2188.

10 S. K. Meher, P. Justin, G. R. Rao, ACS Appl. Mater. Interfaces, 2011, 3, 2063.

11 S. K. Meher, P. Justin, G. R. Rao, Nanoscale, 2011, 3, 683.

12 B. E. Conway, in Electrochemical Supercapacitors, Scientific Fundamentals and Technological Applications, Kluwer Academic/Plenum, New York, 1999.

13 G. S. Gund, D. P. Dubal, S. B. Jambure, S. S. Shinde, C. D. Lokhande, J. Mater. Chem. A, 2013, **1**, 4793.

14 Y. Wang, S. Gai, C. Li, F. He, M. Zhang, Y. Yan, P. Yang, Electrochim. Acta, 2013, **90**, 673.

15 J. Ji, L. L. Zhang, H. Ji, Y. Li, X. Zhao, X. Bai, X. Fan, F. Zhang, R. S. Ruoff, ACS nano, 2013, **7**, 6237.

16 J. Li, F. Luo, X. Tian, Y. Lei, H. Yuan, D. Xiao, J. Power Sources, 2013, **243**, 721.

17 H. Du, L. Jiao, K. Cao, Y. Wang, H. Yuan, ACS Appl. Mater. Interfaces, 2013, **5**, 6643.

18 P. Lu, F. Liu, D. Xue, H. Yang, Y. Liu, Electrochim. Acta, 2012, **78**, 1.

19 Y. Ren, L. Wang, Z. Dai, X. Huang, J. Li, N. Chen, J. Gao, H. Zhao, X. Sun, X. He, Int. J. Electrochem. Sci., 2012, **7**, 12236.

20 M. Aghazadeh, A. N. Golikand, M. Ghaemi, Int. J. Hydrogen Energy, 2011, **36**, 8674.

21 Z. Lu, Z. Chang, W. Zhu, X. Sun, Chem. Commun., 2011, **47**, 9651.

22 U. M. Patil, K. V. Gurav, V. J. Fulari, C. D. Lokhande, O. S. Joo, J. Power Sources, 2009, **188**, 338.

23 Q. Huang, X. Wang, J. Li, C. Dai, S. Gamboa, P. J. Sebastian, J. Power Sources, 2007, **164**, 425.